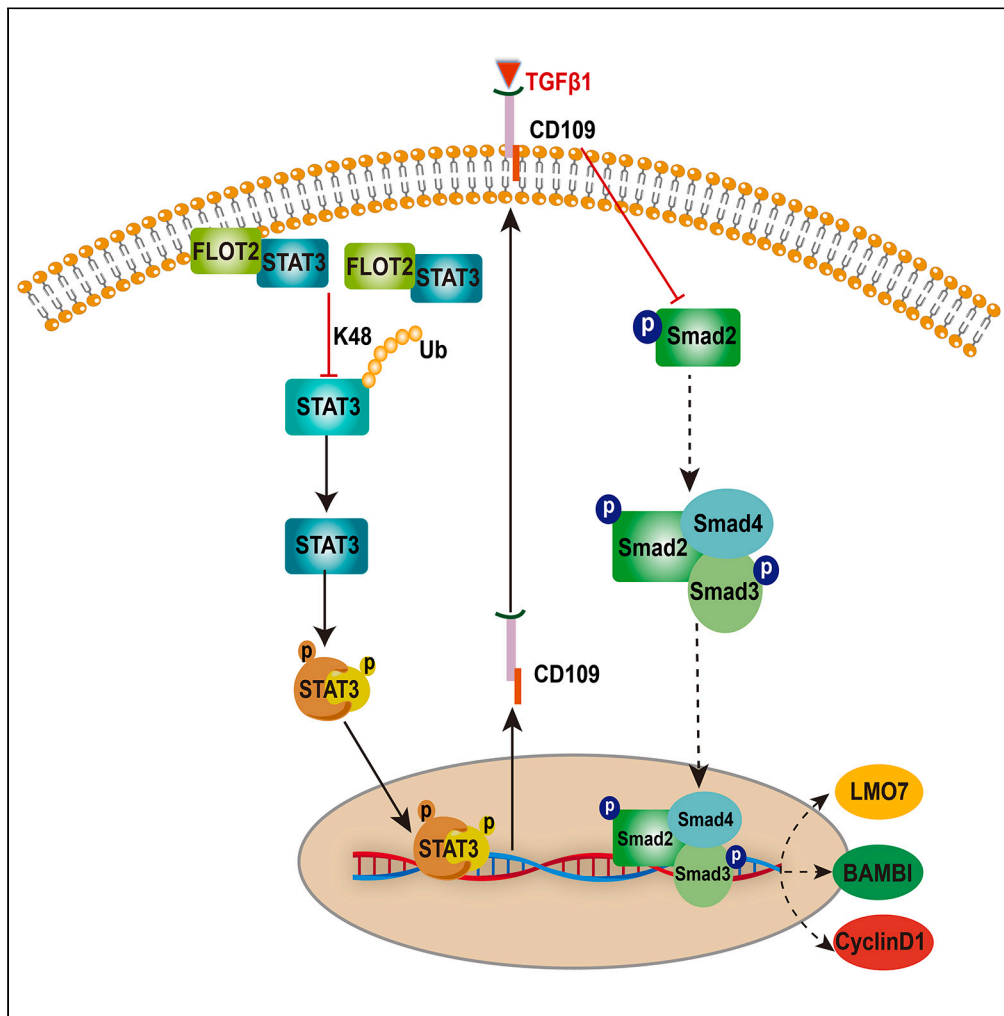


## Article

FLOT2 promotes nasopharyngeal carcinoma progression through suppression of TGF- $\beta$  pathway via facilitating CD109 expression

Hongjuan Xu, Yuze Yin, Yihan Li, ..., Weidong Liu, Xingjun Jiang, Caiping Ren

jiangxj@csu.edu.cn (X.J.)  
rencaiping@csu.edu.cn (C.R.)

## Highlights

FLOT2 negatively regulated the TGF- $\beta$  signal pathway via upregulating CD109 expression

FLOT2 increased the stability of STAT3 by inhibiting K48-linked polyubiquitination

Targeting FLOT2/CD109 axis is a promising therapeutic strategy for NPC therapeutics

## Article

FLOT2 promotes nasopharyngeal carcinoma progression through suppression of TGF- $\beta$  pathway via facilitating CD109 expression

Hongjuan Xu,<sup>1,2,3</sup> Yuze Yin,<sup>1,2,4</sup> Yihan Li,<sup>1,2,4</sup> Ning Shi,<sup>1,2,4</sup> Wen Xie,<sup>1,2,4</sup> Weiren Luo,<sup>5</sup> Lei Wang,<sup>1,2,4</sup> Bin Zhu,<sup>1,2,4</sup> Weidong Liu,<sup>1,2,4</sup> Xingjun Jiang,<sup>2,6,\*</sup> and Caiping Ren<sup>1,2,4,7,\*</sup>

## SUMMARY

**In nasopharyngeal carcinoma (NPC), the TGF- $\beta$ /Smad pathway genes are altered with inactive TGF- $\beta$  signal, but the mechanisms remain unclear. RNA-sequencing results showed that FLOT2 negatively regulated the TGF- $\beta$  signaling pathway via up-regulating CD109 expression. qRT-PCR, western blot, ChIP, and dual-luciferase assays were used to identify whether STAT3 is the activating transcription factor of CD109. Co-IP immunofluorescence staining assays were used to demonstrate the connection between FLOT2 and STAT3. *In vitro* and *in vivo* experiments were used to detect whether CD109 could rescue the functional changes of NPC cells resulting from FLOT2 alteration. IHC and Spearman correlation coefficients were used to assay the correlation between FLOT2 and CD109 expression in NPC tissues. Our results found that FLOT2 promotes the development of NPC by inhibiting TGF- $\beta$  signaling pathway via stimulating the expression of CD109 by stabilizing STAT3, which provides a potential therapeutic strategy for NPC treatment.**

## INTRODUCTION

Nasopharyngeal carcinoma (NPC) is a malignant carcinoma arising from the nasopharyngeal epithelial cells with extremely unbalanced geographical global distribution, which is particularly prevalent in east and southeast Asia accounting for over 70% of new cases of NPC worldwide.<sup>1</sup> Nowadays, intensity-modulated radiotherapy (IMRT), combined with chemoradiotherapy and other treatment methods, has greatly improved the survival of patients with locoregionally advanced NPC (LA-NPC). However, distant metastasis remains the major cause of treatment failure, resulting in deaths from NPC.<sup>2,3</sup> Therefore, it is urgent to clarify the molecular mechanisms underlying NPC growth and metastasis to develop more effective therapies to treat NPC patients.

FLOT2 (flotillin 2, also named reggie-2) is a key component of lipid rafts located in the plasma membrane and is implicated in modulating various biological activities such as signal transduction, actin cytoskeletal organization, neural differentiation, and protein trafficking via interacting with some receptor tyrosine kinases or adhesion molecules.<sup>4–6</sup> Accumulating evidence reveals that elevated expression of FLOT2 can promote cell proliferation, migration, and invasion, and its high expression is associated with cancer progression and poor survival outcomes in a variety of cancers such as breast cancer, non-small cell lung cancer, cervical carcinoma, NPC, and so on.<sup>7–10</sup> In our previous study, we used suppressive subtractive hybridization (SSH) to identify the differential expressed genes between 5-8F (a highly tumorigenic and metastatic NPC cell line) and 6-10B (a tumorigenic and non-metastatic NPC cell line), which were derived from the NPC cell line SUNE1. FLOT2 is one of the most upregulated genes in 5-8F cells compared with 6-10B cells.<sup>11</sup> Our previous results demonstrated that FLOT2 promotes NPC progression by activating NF- $\kappa$ B, PI3K/Akt3, and Wnt pathways in NPC.<sup>12,13</sup> Liu et al. also proved that FLOT2 promotes cell proliferation via activating the c-Myc/BCAT1 axis by suppressing miR-33b-5p in NPC.<sup>10</sup> However, the underlying regulatory mechanisms of FLOT2 involved in NPC progression need to be further elucidated.

Dysregulation of the transforming growth factor  $\beta$  (TGF- $\beta$ )/Smad signaling has been shown to initiate cancer formation and disease progression in various human cancers.<sup>14</sup> In cancers, the TGF- $\beta$  pathway can be either tumor-suppressive or tumor-promoting, depending on the tumor type and stage.<sup>15,16</sup> In NPC, 24.3% of the TGF- $\beta$ /Smad pathway genes are altered with inactive TGF- $\beta$  signal and positive LMP1 status,<sup>17</sup>

<sup>1</sup>NHC Key Laboratory of Carcinogenesis, NHC Key Laboratory of Nanobiological Technology, Department of Neurosurgery, Xiangya Hospital, Central South University, Changsha, Hunan, China

<sup>2</sup>National Clinical Research Center for Geriatric Disorders, Xiangya Hospital, Central South University, Changsha, Hunan, China

<sup>3</sup>Nuclear Medicine (PET Center), Xiangya Hospital, Central South University, Changsha, Hunan, China

<sup>4</sup>The Key Laboratory of Carcinogenesis and Cancer Invasion of the Chinese Ministry of Education, Cancer Research Institute, School of Basic Medical Science, Central South University, Changsha, Hunan, China

<sup>5</sup>Cancer Research Institute, Shenzhen Third People's Hospital, the Second Affiliated Hospital of Southern University of Science and Technology, Shenzhen, Guangdong, China

<sup>6</sup>Department of Neurosurgery, Xiangya Hospital, Central South University, Changsha, China

<sup>7</sup>Lead contact

\*Correspondence: [jiangxj@csu.edu.cn](mailto:jiangxj@csu.edu.cn) (X.J.), [rencaiping@csu.edu.cn](mailto:rencaiping@csu.edu.cn) (C.R.)

<https://doi.org/10.1016/j.isci.2023.108580>



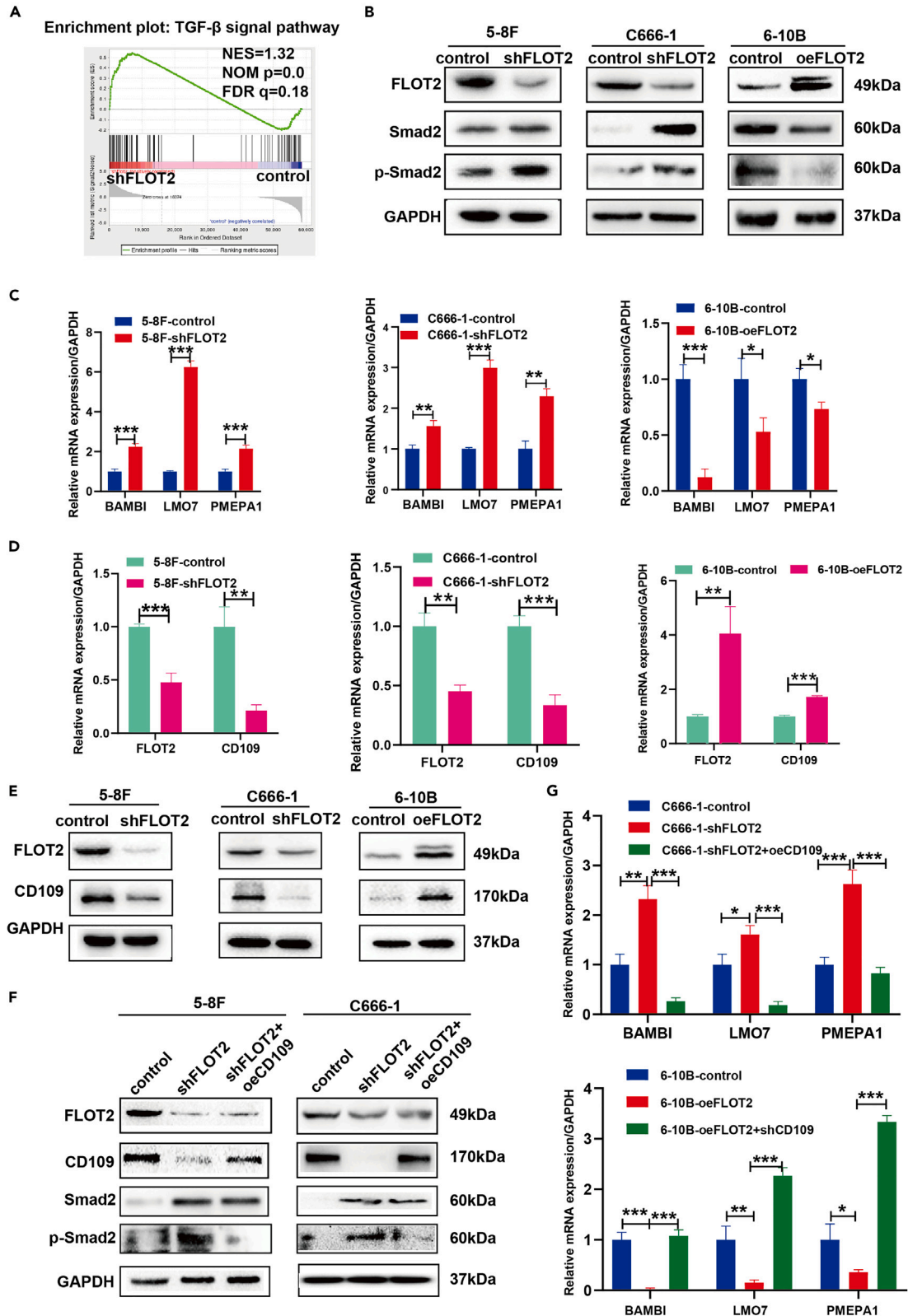


**Figure 1. FLOT2 suppresses TGF- $\beta$  signaling pathway by regulating CD109 expression**

- (A) GSEA profiles showing significant enrichment of TGF- $\beta$  signaling pathway genes in the 5-8F-shFLOT2 group compared with the 5-8F-control group.  
(B) Western blot showed the effects of FLOT2 on Smad2 and p-Smad2 protein levels.  
(C) qRT-PCR was used to assay the effect of FLOT2 on the mRNA level of downstream targets of TGF- $\beta$  pathway.  
(D) qRT-PCR was used to assay the effect of FLOT2 on the mRNA level of CD109.  
(E) Western blot was used to assay the effect of FLOT2 on the protein level of CD109.  
(F) Western blot was used to assay the effect of CD109 on the protein levels of Smad2 and p-Smad2 altered by the changes in FLOT2 expression in NPC cells.  
(G) qRT-PCR was used to assay the effect of CD109 on the mRNA levels of TGF- $\beta$  signal-pathway-related genes altered by the changes in FLOT2 expression in NPC cells. \* $p < 0.05$ ; \*\* $p < 0.01$ ; \*\*\* $p < 0.001$ . Data are represented as mean  $\pm$  SD.

but the mechanisms remain unclear. CD109 belongs to  $\alpha 2$ -macroglobulin/C3, C4, and C5 family of thioester-containing proteins, which has been implicated in several kinds of cancers as an oncogene to drive tumor progression, such as glioblastoma,<sup>18</sup> lung adenocarcinoma,<sup>19</sup> and cervical squamous cell carcinoma.<sup>20</sup> It has been revealed that CD109 promotes the development of cancers via negatively regulating the TGF- $\beta$  signal pathway as the co-receptor of TGF- $\beta$ .<sup>21–23</sup>

In this study, we demonstrated that FLOT2 promoted the NPC progression via negatively regulating TGF- $\beta$  signal pathway. FLOT2 upregulated CD109 expression by stabilizing STAT3. Expression of FLOT2 and CD109 was positively correlated and was significantly higher in NPC tissues than in the normal nasopharyngeal epithelial (NPE) tissues. Our findings provide additional insights into the molecular regulatory network of FLOT2 and provide an experimental basis for exploring the potential of FLOT2 in the diagnosis and treatment of NPC.

**RESULTS****FLOT2 restrains TGF- $\beta$  signaling pathway by regulating CD109 expression**

To investigate the underlying mechanism of FLOT2-mediated tumorigenesis of NPC, we first performed transcriptomic sequencing after the depletion of FLOT2 in 5-8F cells. Gene set enrichment analysis (GSEA) showed that the gene sets of hallmark TGF- $\beta$  targets were enriched in 5-8F-shFLOT2 group, indicating that the TGF- $\beta$  pathway was closely associated with FLOT2 expression (Figure 1A). Western blot results showed that depletion of FLOT2 increased the level of p-Smad2, which is one of the key components of TGF- $\beta$  signal pathway, whereas overexpression of FLOT2 in 6-10B cells resulted in the decreased level of the p-Smad2 (Figure 1B). Meanwhile, FLOT2 silencing increased the expression of p-Smad2 target genes BAMBI, LMO7, and PMEPA1. In contrast, overexpression of FLOT2 led to reduced expression of these genes (Figure 1C). To better assess the involvement of TGF- $\beta$  in FLOT2-elicited tumor proliferation and invasion, we performed CCK8, transwell matrigel invasion, and wound-healing assays using TGF- $\beta$  signaling inhibitor and activator, respectively. Results showed that the TGF- $\beta$  inhibitor SIS3 (10  $\mu$ M, 24 h) treatment could significantly increase the proliferation, invasion, and migration abilities of FLOT2 knockdown NPC cells, whereas recombinant TGF- $\beta$  (5 ng/mL, 24 h) treatment could reduce the effects of FLOT2 overexpression on cell proliferation, invasion, and migration functions of 6-10B cells (Figures S1A–S1C).

To determine the underlying mechanisms by which FLOT2 inhibits the TGF- $\beta$  signal pathway in NPC, we studied the differentially expressed mRNAs between FLOT2-silenced 5-8F cells and 5-8F-control cells associated with the TGF- $\beta$  signal pathway. We found that CD109 was one of the downregulated genes in 5-8F-shFLOT2 cells compared with 5-8F-control cells. Furthermore, qRT-PCR and western blot results demonstrated that both the mRNA and protein levels of CD109 were significantly downregulated in FLOT2 knockdown cells and increased in FLOT2-overexpressed cells (Figures 1D and 1E), suggesting that FLOT2 positively regulates CD109 expression. Meanwhile, western blot results showed that CD109 was also upregulated in 5-8F cells compared with 6-10B cells, which was the same trend as FLOT2 in 5-8F and 6-10B cells (Figure S2A). Importantly, CD109 has been reported to negatively regulate TGF- $\beta$  signaling pathway. Therefore, we speculated that FLOT2 inactivates TGF- $\beta$  signal pathway by enhancing CD109 expression in NPC. As expected, CD109 overexpression suppressed the protein levels of p-Smad2 and its target genes in FLOT2 knockdown cells, whereas CD109 knockdown increased the protein levels of p-Smad2 and its target genes in FLOT2 overexpression cells, indicating that CD109 was responsible for FLOT2-mediated inactivation of TGF- $\beta$  signaling pathway (Figures 1F and 1G).

**FLOT2 upregulates CD109 expression via STAT3**

Next, we explored the mechanism by which FLOT2 regulates CD109 expression in NPC. As both FLOT2 and CD109 are membrane proteins, we first investigated whether both of them could form complexes. Immunofluorescence staining assay results displayed that there was a co-location between FLOT2 and CD109 in NPC cells (Figure S2B). However, Co-IP results showed that there was no direct interaction between FLOT2 and CD109 in 5-8F and C666-1 cells (Figure S2C). Therefore, FLOT2 and CD109 did not form complexes in NPC cells, and we considered that FLOT2 may regulate CD109 expression at the transcriptional level.

We focused on searching for an important transcription factor that was affected by FLOT2. Several studies reminded us that lipid-raft-associated proteins had interactions with STAT3 pathway,<sup>24,25</sup> so we presumed that FLOT2 might function through STAT3. Western blot results showed that the knockdown of FLOT2 reduced the protein level of CD109, STAT3, and p-STAT3. Conversely, overexpression of FLOT2 increased the protein level of CD109, STAT3, and p-STAT3 (Figure 2A). Meanwhile, overexpression of STAT3 in FLOT2-silenced NPC cells increased the mRNA and protein levels of CD109. On the contrary, silencing of STAT3 in FLOT2-overexpressed NPC cells decreased the mRNA and protein levels of CD109 (Figures 2B and 2C). Furthermore, qRT-PCR and western blot assays showed that the mRNA and protein

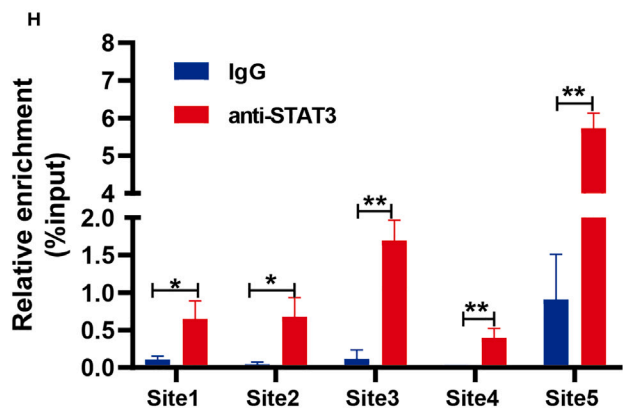
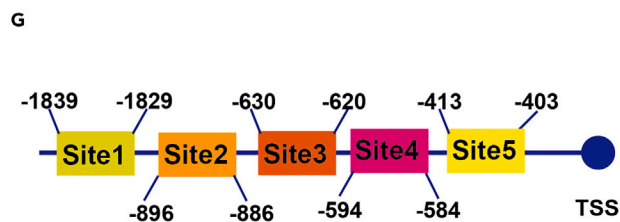
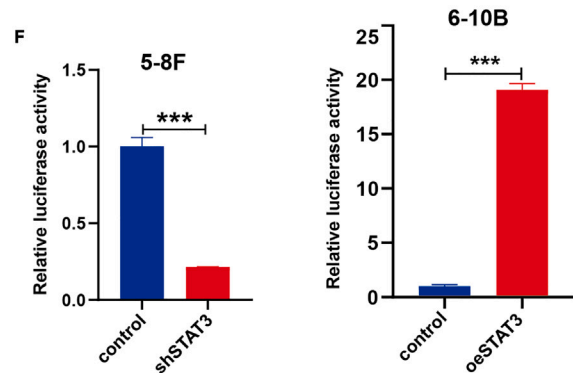
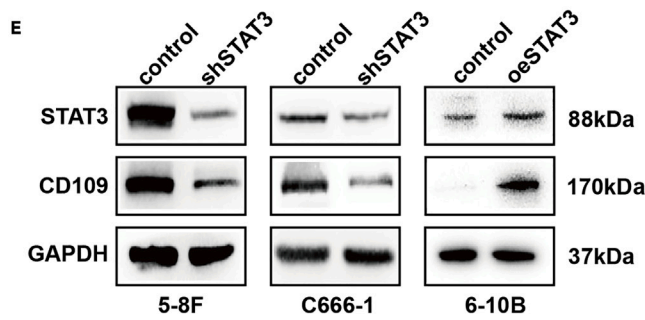
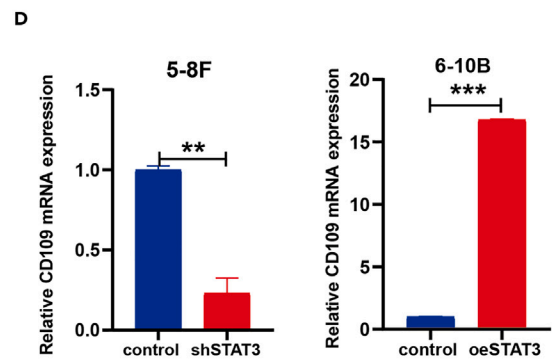
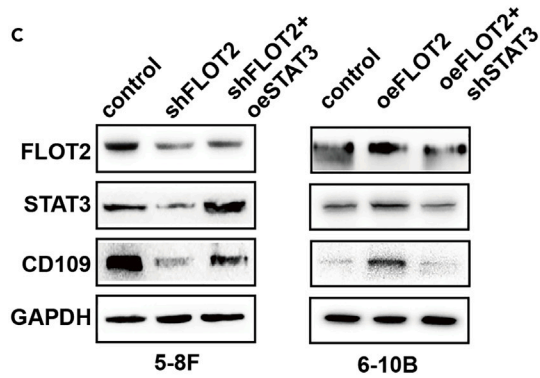
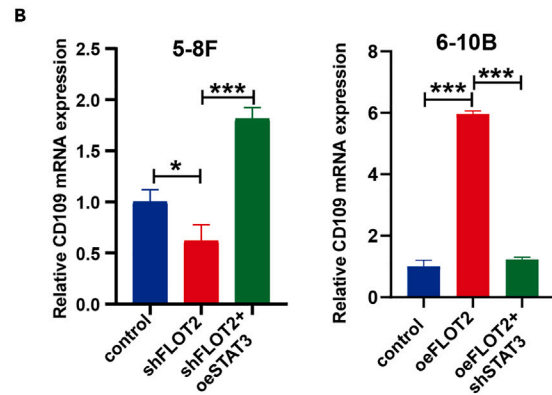
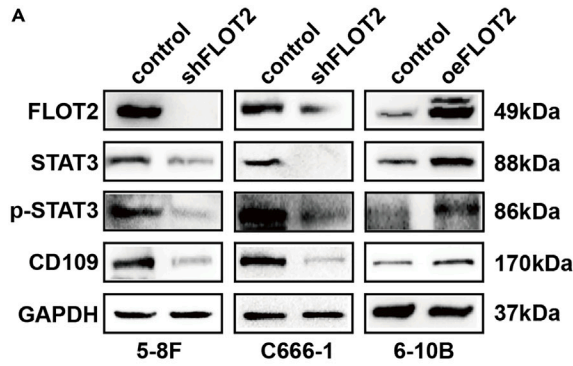


**Figure 2. FLOT2 upregulates CD109 expression via STAT3**

- (A) Western blot analysis was used to detect the effect of FLOT2 on CD109 and STAT3 protein levels.  
(B) qRT-PCR was used to detect whether STAT3 could rescue the mRNA level of CD109 altered by the changes in FLOT2 expression in NPC cells.  
(C) Western blot analysis was used to detect whether STAT3 could rescue the protein level of CD109 altered by the changes in FLOT2 expression in NPC cells.  
(D) qRT-PCR was used to detect the effect of STAT3 on CD109 mRNA levels.  
(E) Western blot analysis was used to detect the effect of STAT3 on CD109 protein levels.  
(F) The dual-luciferase assay was used to test the CD109 promoter activity in NPC cells due to STAT3 expression changes.  
(G) JASPAR predicted the potential binding sites of STAT3 in the CD109 promoter.  
(H) ChIP-PCR was used to detect the binding sites of STAT3 in the CD109 promoter. \* $p < 0.05$ ; \*\* $p < 0.01$ ; \*\*\* $p < 0.001$ . Data are represented as mean  $\pm$  SD.

levels of CD109 were reduced after the expression of STAT3 was downregulated, whereas the mRNA and protein levels of CD109 were increased after the expression of STAT3 was upregulated (Figures 2D and 2E). Subsequently, we conducted the luciferase reporter assays. Depletion of STAT3 significantly reduced the activity of the CD109 promoter in 5-8F cells, whereas overexpression of STAT3 enhanced the activity of the CD109 promoter in 6-10B cells (Figure 2F). Next, we searched the binding sites of STAT3 to the promoter region of CD109. With the use of JASPAR and UCSC online tools, we identified five possible STAT3 binding sites in the promoter region of CD109 (Figure 2G). Consistently, the ChIP-PCR assay showed that STAT3 could directly bind to CD109 promoter regions at the five sites (Figure 2H).

**FLOT2 stabilizes STAT3 in NPC cells**

To explore the mechanism by which FLOT2 regulates the expression of STAT3, we performed a Co-IP experiment using cell lysates from 5-8F, C666-1, and 6-10B cells, and the results revealed endogenous interactions between FLOT2 and STAT3 in these three cell lines (Figure 3A). Meanwhile, pLV-FLOT2, pEnter-STAT3-His plasmids were co-transfected into HEK293T cells, and Co-IP results demonstrated that exogenous STAT3 also interacted with exogenous FLOT2 (Figure 3B). Immunofluorescence staining assay also confirmed the colocalization between FLOT2 and STAT3 in the NPC cells, mainly in the cytoplasm (Figure 3C). Collectively, these results provided strong experimental evidence that STAT3 interacts with FLOT2. We then tested the effect of FLOT2/STAT3 interaction on STAT3 protein stability after blocking protein synthesis by incubating cells with 50  $\mu$ M of cycloheximide (CHX). The protein level of STAT3 decreased more quickly in the FLOT2 knockdown NPC cells than in control NPC cells during CHX incubation (Figure 3D), and the rate of STAT3 decline was much faster in shFLOT2 cells than in control cells (Figure 3E), suggesting that FLOT2 affects the stability of STAT3 protein. Furthermore, the reduction of STAT3 protein in the FLOT2 knockdown cells was significantly reversed after treating the cells with proteasome inhibitor MG132 (Figure 3F), indicating a proteasome-dependent way in STAT3 destabilization with FLOT2 depletion. We then investigated how FLOT2 improves STAT3 stability. As the ubiquitin-proteasome system is one of the protein degradation pathways,<sup>26</sup> we then investigated the ability of FLOT2 to regulate STAT3 ubiquitination and discovered that FLOT2 knockdown enhanced STAT3 polyubiquitination, whereas FLOT2 overexpression reduced STAT3 polyubiquitination level in the NPC cells (Figure 3G), indicating that FLOT2 upregulates STAT3 stabilization by suppressing its polyubiquitination degradation. K48-linked and K63-associated polyubiquitination are the two main forms of protein ubiquitination; K48-mediated ubiquitin leads to proteasomal degradation of target proteins, and K63 usually modulates protein function, cell signaling, and DNA damage repair.<sup>27</sup> Therefore, we investigated the type of the FLOT2-mediated STAT3 polyubiquitin chains in the HEK293T cells simultaneously transfected with the combinations of plasmids expressing FLOT2, STAT3, HA-Ub, HA-UbK48, and HA-UbK63. Our results demonstrated that the K48-linked ubiquitination of STAT3 was obviously downregulated by FLOT2, suggesting that FLOT2 inhibits the K48-linked polyubiquitination of STAT3. Meanwhile, FLOT2 also enhanced the K63-linked ubiquitination of STAT3 (Figure 3H). Together, these results indicate that the direct binding of FLOT2 to STAT3 enhances STAT3 stability by suppressing its ubiquitination-proteasome degradation in NPC cells.

**FLOT2 promotes NPC progression by upregulating CD109 *in vitro* and *in vivo***

Based on the abovementioned experiments, we found that CD109 was regulated by FLOT2 via STAT3. Thus, we analyzed whether CD109 would reverse the effects of altered FLOT2 expression on the biological phenotypes of NPC cells. FLOT2 knockdown cells were transfected with CD109 expression plasmids. The results showed that CD109 expression significantly increased the proliferation, cell cycle transition, migration, and invasion abilities of FLOT2 knockdown NPC cells (Figures 4A–4G), whereas CD109 knockdown weakened the effects of FLOT2 overexpression on cell proliferation and invasion functions of 6-10B cells (Figures 4A and S3A–S3C).

To investigate whether FLOT2 could promote tumor proliferation and metastasis through CD109 *in vivo*, the subcutaneous NPC-bearing mouse model and tail intravenous lung metastasis mouse model were established. The results showed that depletion of FLOT2 significantly inhibited the growth of tumor cells in nude mice, whereas CD109 overexpression reversed the growth-inhibiting effect of FLOT2 depletion on the tumor cells in nude mice (Figures 5A–5C). The IHC experiment results showed that FLOT2, CD109, and Ki67 expression in the FLOT2 depletion group was significantly lower than that in the control group, whereas in the shFLOT2 and overexpressing CD109 group, the expression level of Ki67 was higher than that in the shFLOT2 group (Figure 5D). In the metastatic models, the number of nodules was significantly reduced due to the knockdown of FLOT2 expression compared with the control group, whereas overexpression of CD109 in the shFLOT2 group increased the number of nodules (Figures 5E–5G). These results suggest that FLOT2 can promote tumor proliferation and metastasis by upregulating CD109 *in vivo*.

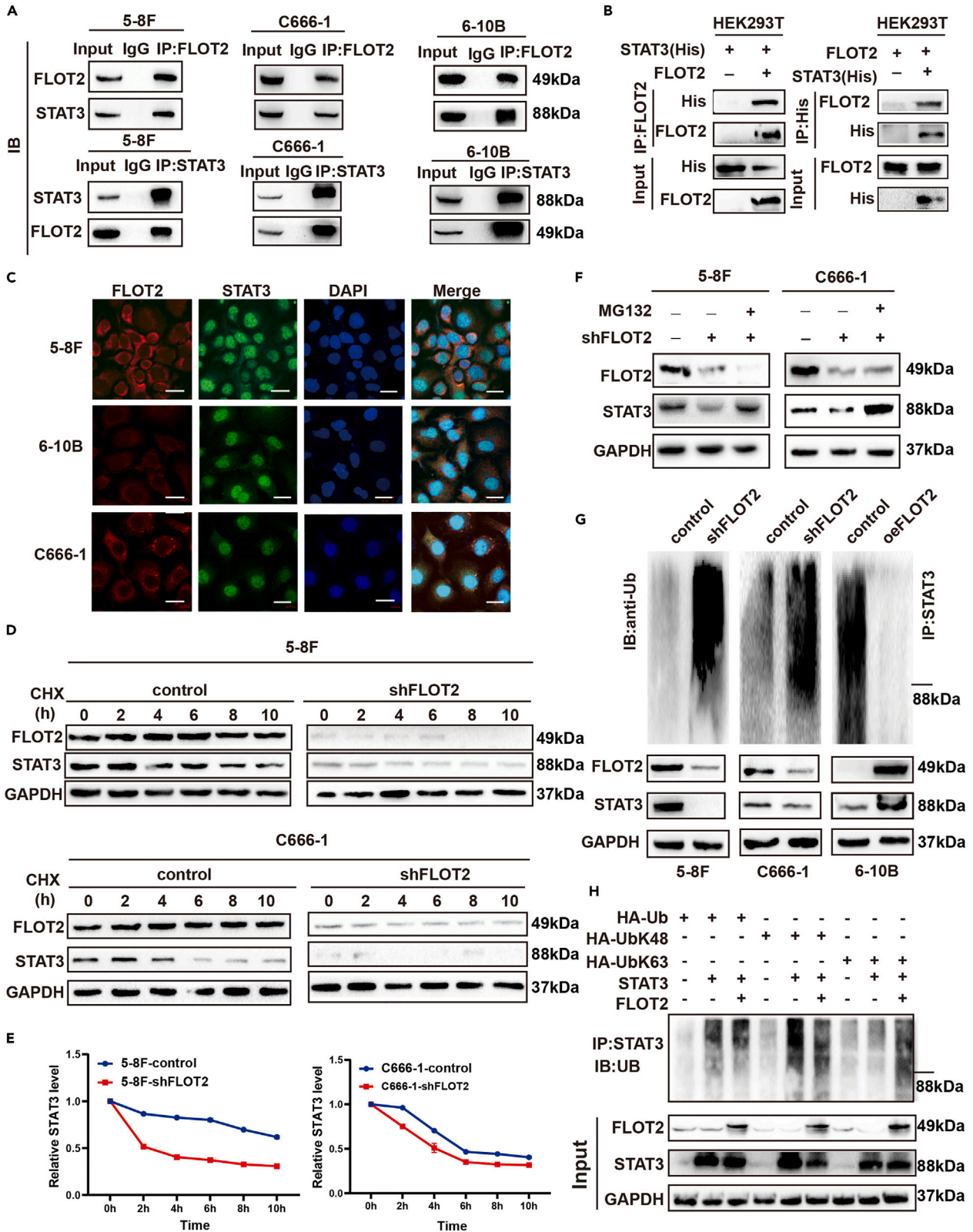


**Figure 3. FLOT2 regulates the protein level of STAT3**

- (A) Co-IP assay was used to evaluate the interaction of endogenous FLOT2 and STAT3 in NPC cells.
- (B) Co-IP was used to evaluate the interaction of exogenous FLOT2 and STAT3 in the HEK293T cells ectopically expressing FLOT2 and His-tagged STAT3.
- (C) Immunofluorescent staining was used to evaluate the colocalization of FLOT2 (red) and STAT3 (green) in NPC cells. Scale bar, 20  $\mu\text{m}$ .
- (D) Western blot analysis was used to detect the effect of FLOT2 expression changes on STAT3 protein stability in the NPC cells treated with 50  $\mu\text{g}/\text{mL}$  cycloheximide for indicated times.
- (E) The degradation rate of STAT3 was calculated with gray analysis.
- (F) Western blot analysis showed the effect of FLOT2 knockdown on ubiquitin-proteasome-mediated protein stability of STAT3 in MG132-treated NPC cells.
- (G) Co-IP was used to evaluate the effect of FLOT2 expression changes on STAT3 polyubiquitination in NPC cells.
- (H) Co-IP was used to evaluate the type of effect of FLOT2 on STAT3 polyubiquitination. Total cell proteins extracted from HEK293T cells transfected with indicated plasmids and treated with 20  $\mu\text{mol}/\text{L}$  MG132 for 6 h underwent IP with anti-STAT3 antibody, followed by western blot analysis with anti-polyubiquitin antibody.

**FLOT2 and CD109 are positively correlated in NPC clinical samples**

We then investigated the correlations of FLOT2 and CD109 in NPC clinical samples. Firstly, by analyzing the GEO batch (61 NPC samples), we found that FLOT2 was positively correlated with CD109 in NPC samples ( $r = 0.4122$ ;  $p < 0.001$ ) (Figure 6A). IHC results also showed both FLOT2 and CD109 protein levels were higher in NPC tissues compared with those in NPE tissues (Figure 6B). Our previous work has shown that NPC patients with high expression of FLOT2 had reduced OS and DFS. Here, we showed that NPC patients with high expression of CD109 also had reduced OS and DFS (Figure 6C). Meanwhile, NPC patients with high expression of both FLOT2 and CD109 showed more significantly reduced OS and DFS compared with patients with high levels of only one of the two proteins (Figure 6D).

**DISCUSSION**

In this study, we found that FLOT2 negatively regulated TGF- $\beta$  signal pathway by activating the expression of CD109 in NPC. FLOT2 upregulated the expression of CD109 via stabilizing STAT3. CD109 overexpression or knockdown could rescue the changes in proliferation, cell cycle transition, and metastasis abilities of NPC cells caused by FLOT2 knockdown or overexpression both *in vitro* and *in vivo*. Patients with high expression of both FLOT2 and CD109 presented poorer OS and DFS than those with high expression of one protein alone. Supported by the experimental data, our results provided new therapeutic targets in carcinogenesis in NPC.

Nowadays, more and more studies have identified the mechanisms of FLOT2 in tumor progression. Several studies found that FLOT2 promotes tumor progression via activating the MEK/ERK, AKT, Wnt, and NF- $\kappa\text{B}$  pathways,<sup>28</sup> all of which are critical pathways in cancer progression. As one of the lipid-raft-associated proteins, FLOT2 can interact with different molecules to modulate numerous biological processes, including tumor cell proliferation, migration, and invasion as well as viral infection and cancer metastasis.<sup>29,30</sup> In this study, we showed that FLOT2 interacts and positively correlates with STAT3 and maintains the stability of STAT3, which accounts for the upregulation of CD109 in NPC. STAT3 is the activating transcription factor of CD109, which can bind to the promoter region of CD109 directly. Previous studies reported that CD109 promoted cancer progression via activating STAT3 signaling. Filppu et al. found that CD109 physically interacts with glycoprotein 130, which is required for activation of the IL-6/STAT3 pathway to maintain the self-renewal and tumorigenicity of glioblastoma stem cells.<sup>18</sup> Chuang et al. also showed that CD109 promoted metastasis of lung adenocarcinoma via JAK/STAT3 pathway.<sup>31</sup> CD109 promotes tumorigenicity and cancer aggressiveness via the EGFR/STAT3 axis in cervical squamous cell carcinoma.<sup>20</sup> CD109 plays an important role in the acquisition of drug resistance via activating the STAT3-NOTCH1 signaling axis in patients with epithelial ovarian cancer.<sup>32</sup> Therefore, we speculate that a positive feedback loop exists between CD109 and STAT3. STAT3 is abnormally activated in multiple human tumors, including NPC,<sup>33</sup> and regulates the transcription of many key genes related to proliferation, metastasis, drug resistance, and immune suppression of tumor cells.<sup>34</sup> In this paper, our results showed that FLOT2 enhances STAT3 stability by suppressing its ubiquitination-proteasome degradation in NPC cells, so our results reveal one molecular mechanism that modulation of STAT3 activation at a post-translational level through ubiquitination regulation.

TGF- $\beta$  signal pathway plays a critical role in carcinogenesis. It has dual functions as a tumor suppressor that inhibits cell-cycle conversion from the G1 to S phase and activates cell apoptosis, senescence, and differentiation at the early stage and a tumor promoter in the later phases of disease that induces tumor cell migration, invasion, epithelial-to-mesenchymal transition (EMT), and metastasis.<sup>35</sup> In this study, RNA sequencing (GEO database: dataset GSE245418) and qRT-PCR results revealed that FLOT2 negatively regulates the TGF- $\beta$  signal pathway in NPC 5-8F cells. FLOT2 downregulates a series of TGF- $\beta$ -relevant genes related to tumor suppression, such as PMEPA1, BAMBI, and LMO7. BAMBI suppresses NPC progression as one of the target genes of the canonical TGF- $\beta$  signaling.<sup>36</sup> Previous studies demonstrated that CD109 serves as a TGF- $\beta$  co-receptor and inhibits TGF- $\beta$  signaling in keratinocytes and human cancers.<sup>23,37</sup> Mechanically, CD109 attenuates TGF- $\beta$ -signaling-induced Smad2/3 phosphorylation via promoting degradation of TGF- $\beta$  receptors.<sup>38–40</sup>

In summary, FLOT2 promotes NPC progression via FLOT2/STAT3/CD109 axis. Targeting FLOT2 alone or in combination with other targets may be a promising therapeutic strategy for the treatment of NPC.

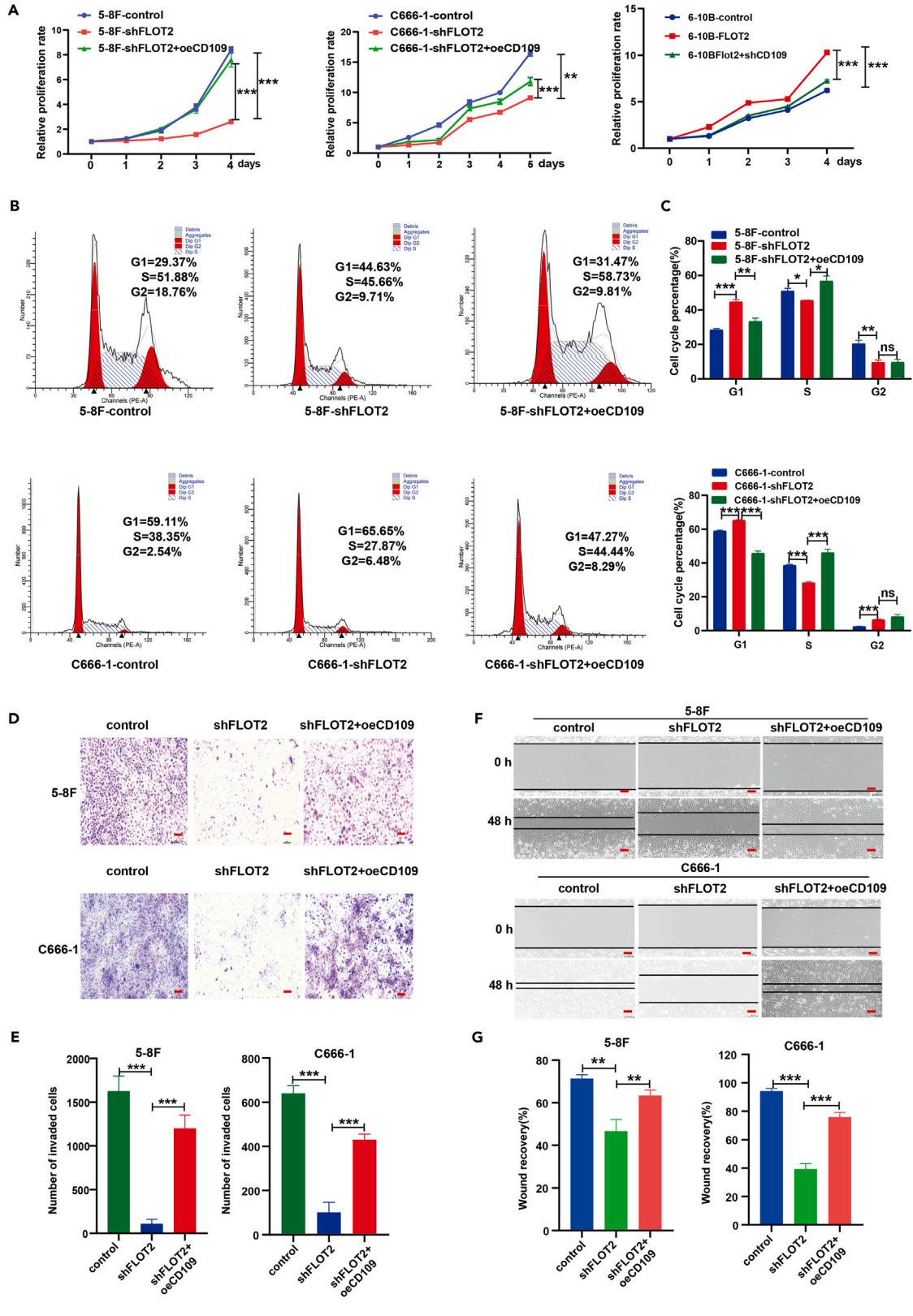


**Figure 4. CD109 rescues the effects of altered FLOT2 expression on NPC cells *in vitro***

(A) The cell viability of NPC cells was evaluated by the CCK-8 method.

(B and C) The cell cycle of NPC cells was evaluated by flow cytometry.

(D and E) The cell invasion ability of NPC cells was tested by the matrigel invasion analysis. Scale bar, 100  $\mu$ m.

(F and G) The cell migration ability of NPC cells was evaluated with the scratch wound healing analysis. Scale bar, 100  $\mu$ m. \*\*p < 0.01; \*\*\*p < 0.001. Data are represented as mean  $\pm$  SD.

**Limitations of the study**

FLOT2 was upregulated in NPC tissues, especially in metastatic nasopharyngeal carcinoma, but we did not study the mechanisms of the up-regulation of FLOT2 in NPC. Our study only introduced the mechanisms of FLOT2 regulating the protein level of p-smad2 in NPC cells, and it is necessary to further clarify how FLOT2 regulated the expression of Smad2. We need to search for one ubiquitination-related protein that is involved in the stabilization of STAT3 induced by FLOT2.

**STAR★METHODS**

Detailed methods are provided in the online version of this paper and include the following:

- KEY RESOURCES TABLE
- RESOURCE AVAILABILITY
  - Lead contact
  - Materials availability
  - Data and code availability
- EXPERIMENTAL MODEL AND STUDY PARTICIPANT DETAILS
  - Clinical samples
  - *In vivo* experiments
- METHOD DETAILS
  - Cell culture, transfection, and treatment
  - Immunohistochemistry (IHC) and Hematoxylin and eosin (HE)
  - Cell viability assay
  - Cell cycle analysis by flow cytometry
  - Transwell matrigel invasion and wound-healing assays
  - Quantitative real-time polymerase chain reaction (qRT-PCR)
  - Western blot analysis
  - Co-immunoprecipitation (Co-IP) assay
  - Immunofluorescence staining
  - Chromatin immunoprecipitation (ChIP) assay
  - Dual-luciferase assay
  - RNA sequencing
- QUANTIFICATION AND STATISTICAL ANALYSIS

**SUPPLEMENTAL INFORMATION**

Supplemental information can be found online at <https://doi.org/10.1016/j.isci.2023.108580>.

**ACKNOWLEDGMENTS**

This work was supported by the National Natural Science Foundation of China (No. 81773179, 82071399, 82303533), the Key Research and Development Program of Hunan (2022SK2055), the Natural Science Foundation of Hunan Province (2022JJ30931, 2023JJ30733, 2023JJ41007), the Natural Science Foundation of Changsha City (kq2208397), the Natural Science Foundation of Shenzhen (JCYJ20190809154603583, JCYJ20210324131210030), and the Youth Science Foundation of Xiangya Hospital (2022Q18).

**AUTHOR CONTRIBUTIONS**

X.J. and C.R. designed the experiments. H.X. performed the experiments, prepared figures, and drafted the manuscript. Y.Y., Y.L., and Y.Z. collected the clinical samples and analyzed the data. L.W. and B.Z. supervised laboratory processes. H.X., W.L., X.J., and C.R. provided the research fund. W.L. and C.R. provided the revision proposal. All authors read and approved the final manuscript.

**DECLARATION OF INTERESTS**

The authors declare no competing interests.

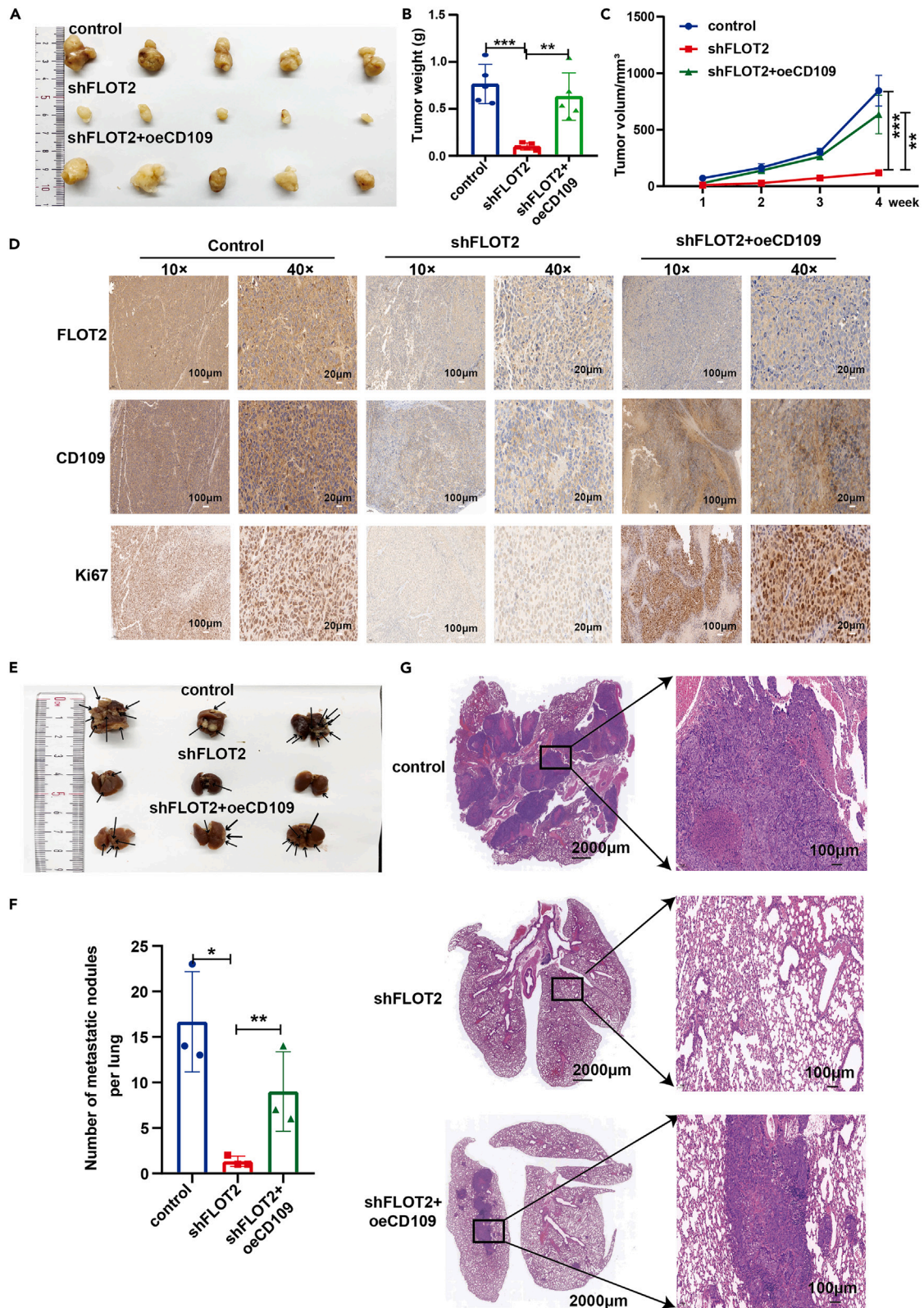


**Figure 5. CD109 reverses the suppressive effect of FLOT2 knockdown on tumor growth and lung metastasis *in vivo***

- (A) Macroscopic view of xenograft tumors from 5-8F-control, 5-8F-shFLOT2, and 5-8F-shFLOT2+oeCD109 groups.  
 (B) Tumor weight.  
 (C) Tumor volume.  
 (D) Immunohistochemical staining of FLOT2, CD109, and Ki67 proteins in tumor tissues. Scale bar, 100  $\mu\text{m}$  (10 $\times$ ), 20  $\mu\text{m}$  (40 $\times$ ).  
 (E) Macroscopic view of mouse lung tissues from the metastatic tumor model.  
 (F) The number of metastatic lung nodules from the 5-8F-control, 5-8F-shFLOT2, and 5-8F-shFLOT2+oeCD109 groups.  
 (G) Representative images of lung metastasis samples from 5-8F-control, 5-8F-shFLOT2, and 5-8F-shFLOT2+oeCD109 groups by HE staining. \* $p < 0.05$ ; \*\* $p < 0.01$ ; \*\*\* $p < 0.001$ . Data are represented as mean  $\pm$  SD.

Received: July 10, 2023

Revised: September 28, 2023

Accepted: November 23, 2023

Published: November 25, 2023

**REFERENCES**

- Chen, Y.-P., Chan, A.T.C., Le, Q.-T., Blanchard, P., Sun, Y., and Ma, J. (2019). Nasopharyngeal carcinoma. *Lancet* 394, 64–80.
- Hong, X., Liu, N., Liang, Y., He, Q., Yang, X., Lei, Y., Zhang, P., Zhao, Y., He, S., Wang, Y., et al. (2020). Circular RNA CRIM1 functions as a ceRNA to promote nasopharyngeal carcinoma metastasis and docetaxel chemoresistance through upregulating FOXQ1. *Mol. Cancer* 19, 33.
- Chen, Y., Zhao, Y., Yang, X., Ren, X., Huang, S., Gong, S., Tan, X., Li, J., He, S., Li, Y., et al. (2022). USP44 regulates irradiation-induced DNA double-strand break repair and suppresses tumorigenesis in nasopharyngeal carcinoma. *Nat. Commun.* 13, 501.
- Huang, W., Xiong, Q., Lin, M., and Rikihisa, Y. (2021). Anaplasma phagocytophilum Hijacks Flotillin and NPC1 Complex To Acquire Intracellular Cholesterol for Proliferation, Which Can Be Inhibited by Ezetimibe. *mBio* 12, e0229921.
- Hanafusa, K., and Hayashi, N. (2019). The Flot2 component of the lipid raft changes localization during neural differentiation of P19C6 cells. *BMC Mol. Cell Biol.* 20, 38.
- Xiong, Q., Lin, M., Huang, W., and Rikihisa, Y. (2019). Infection by Anaplasma phagocytophilum Requires Recruitment of Low-Density Lipoprotein Cholesterol by Flotillins. *mBio* 10, e02783-18.
- Wang, X., Yang, Q., Guo, L., Li, X.-H., Zhao, X.-H., Song, L.-B., and Lin, H.-X. (2013). Flotillin-2 is associated with breast cancer progression and poor survival outcomes. *J. Transl. Med.* 11, 190.
- Wang, Y.-L., Yao, W.-J., Guo, L., Xi, H.-F., Li, S.-Y., and Wang, Z.-M. (2015). Expression of flotillin-2 in human non-small cell lung cancer and its correlation with tumor progression and patient survival. *Int. J. Clin. Exp. Pathol.* 8, 601–607.
- Liu, Y., Lin, L., Huang, Z., Ji, B., Mei, S., Lin, Y., and Shen, Z. (2015). High expression of flotillin-2 is associated with poor clinical survival in cervical carcinoma. *Int. J. Clin. Exp. Pathol.* 8, 622–628.
- Liu, R., Liu, J., Wu, P., Yi, H., Zhang, B., and Huang, W. (2021). Flotillin-2 promotes cell proliferation via activating the c-Myc/BCAT1 axis by suppressing miR-33b-5p in nasopharyngeal carcinoma. *Aging (Albany NY)* 13, 8078–8094.
- Yang, X.-Y., Ren, C.-P., Wang, L., Li, H., Jiang, C.-J., Zhang, H.-B., Zhao, M., and Yao, K.-T. (2005). Identification of differentially expressed genes in metastatic and non-metastatic nasopharyngeal carcinoma cells by suppression subtractive hybridization. *Cell. Oncol.* 27, 215–223.
- Liu, J., Huang, W., Ren, C., Wen, Q., Liu, W., Yang, X., Wang, L., Zhu, B., Zeng, L., Feng, X., et al. (2015). Flotillin-2 promotes metastasis of nasopharyngeal carcinoma by activating NF- $\kappa$ B and PI3K/Akt3 signaling pathways. *Sci. Rep.* 5, 11614.
- Xu, H., Yan, X., Zhu, H., Kang, Y., Luo, W., Zhao, J., Zhou, K., Liu, X., Ye, L., Zhou, Q., et al. (2022). TBL1X and Flot2 form a positive feedback loop to promote metastasis in nasopharyngeal carcinoma. *Int. J. Biol. Sci.* 18, 1134–1149.
- Wu, M.-Z., Yuan, Y.-C., Huang, B.-Y., Chen, J.-X., Li, B.-K., Fang, J.-H., and Zhuang, S.-M. (2021). Identification of a TGF- $\beta$ /SMAD/Inc-UTGF positive feedback loop and its role in hepatoma metastasis. *Signal Transduct. Target. Ther.* 6, 395.
- Gungor, M.Z., Uysal, M., and Senturk, S. (2022). The Bright and the Dark Side of TGF- $\beta$  Signaling in Hepatocellular Carcinoma: Mechanisms, Dysregulation, and Therapeutic Implications. *Cancers* 14, 940.
- Ciardello, D., Elez, E., Taberner, J., and Seoane, J. (2020). Clinical development of therapies targeting TGF $\beta$ : current knowledge and future perspectives. *Ann. Oncol.* 31, 1336–1349.
- Bruce, J.P., To, K.-F., Lui, V.W.Y., Chung, G.T.Y., Chan, Y.-Y., Tsang, C.M., Yip, K.Y., Ma, B.B.Y., Woo, J.K.S., Hui, E.P., et al. (2021). Whole-genome profiling of nasopharyngeal carcinoma reveals viral-host co-operation in inflammatory NF- $\kappa$ B activation and immune escape. *Nat. Commun.* 12, 4193.
- Filppu, P., Tanjore Ramanathan, J., Granberg, K.J., Gucciardo, E., Haapasalo, H., Lehti, K., Nykter, M., Le Joncour, V., and Laakkonen, P. (2021). CD109-GP130 interaction drives glioblastoma stem cell plasticity and chemoresistance through STAT3 activity. *JCI Insight* 6, e141486.
- Lee, K.-Y., Kuo, T.-C., Chou, C.-M., Hsu, W.-J., Lee, W.-C., Dai, J.-Z., Wu, S.-M., and Lin, C.-W. (2020). Upregulation of CD109 Promotes the Epithelial-to-Mesenchymal Transition and Stemness Properties of Lung Adenocarcinomas via Activation of the Hippo-YAP Signaling. *Cells* 10, 28.
- Mo, X.-T., Leung, T.H.-Y., Tang, H.W.-M., Siu, M.K.-Y., Wan, P.K.-T., Chan, K.K.-L., Cheung, A.N.-Y., and Ngan, H.Y.-S. (2020). CD109 mediates tumorigenicity and cancer aggressiveness via regulation of EGFR and STAT3 signalling in cervical squamous cell carcinoma. *Br. J. Cancer* 123, 833–843.
- Taki, T., Shiraki, Y., Enomoto, A., Weng, L., Chen, C., Asai, N., Murakumo, Y., Yokoi, K., Takahashi, M., and Mii, S. (2020). CD109 regulates *in vivo* tumor invasion in lung adenocarcinoma through TGF- $\beta$  signaling. *Cancer Sci.* 111, 4616–4628.
- Pawlak, J.B., and Blobel, G.C. (2022). TGF- $\beta$  superfamily co-receptors in cancer. *Dev. Dyn.* 251, 137–163.
- Tanabe, M., Hosokawa, K., Nguyen, M.A.T., Nakagawa, N., Maruyama, K., Tsuji, N., Urushihara, R., Espinoza, L., Elbadry, M.I., Mohiuddin, M., et al. (2022). The GPI-anchored protein CD109 protects hematopoietic progenitor cells from undergoing erythroid differentiation induced by TGF- $\beta$ . *Leukemia* 36, 847–855.
- Liu, Y., Yan, G., Gao, M., and Zhang, X. (2018). Magnetic capture of polydopamine-encapsulated HeLa cells for the analysis of cell surface proteins. *J. Proteomics* 172, 76–81.
- Lee, M.Y., Ryu, J.M., Lee, S.H., Park, J.H., and Han, H.J. (2010). Lipid rafts play an important role for maintenance of embryonic stem cell self-renewal. *J. Lipid Res.* 51, 2082–2089.
- Rousseau, A., and Bertolotti, A. (2018). Regulation of proteasome assembly and activity in health and disease. *Nat. Rev. Mol. Cell Biol.* 19, 697–712.
- Madiraju, C., Novack, J.P., Reed, J.C., and Matsuzawa, S.-I. (2022). K63 ubiquitination in immune signaling. *Trends Immunol.* 43, 148–162.
- Li, Y., and Dou, S. (2022). FLOT2 Promotes the Proliferation and Epithelial-mesenchymal Transition of Cervical Cancer by Activating the MEK/ERK1/2 Pathway. *Balkan Med. J.* 39, 267–274.
- Liu, W., Liu, X., Wang, L., Zhu, B., Zhang, C., Jia, W., Zhu, H., Liu, X., Zhong, M., Xie, D., et al. (2018). PLCD3, a flotillin2-interacting protein, is involved in proliferation, migration and invasion of nasopharyngeal carcinoma cells. *Oncol. Rep.* 39, 45–52.
- Song, T., Hu, Z., Liu, J., and Huang, W. (2021). FLOT2 upregulation promotes growth and invasion by interacting and stabilizing EphA2 in gliomas. *Biochem. Biophys. Res. Commun.* 548, 67–73.
- Chuang, C.-H., Greenside, P.G., Rogers, Z.N., Brady, J.J., Yang, D., Ma, R.K., Caswell, D.R., Chiou, S.-H., Winters, A.F., Grüner, B.M., et al. (2017). Molecular definition of a metastatic

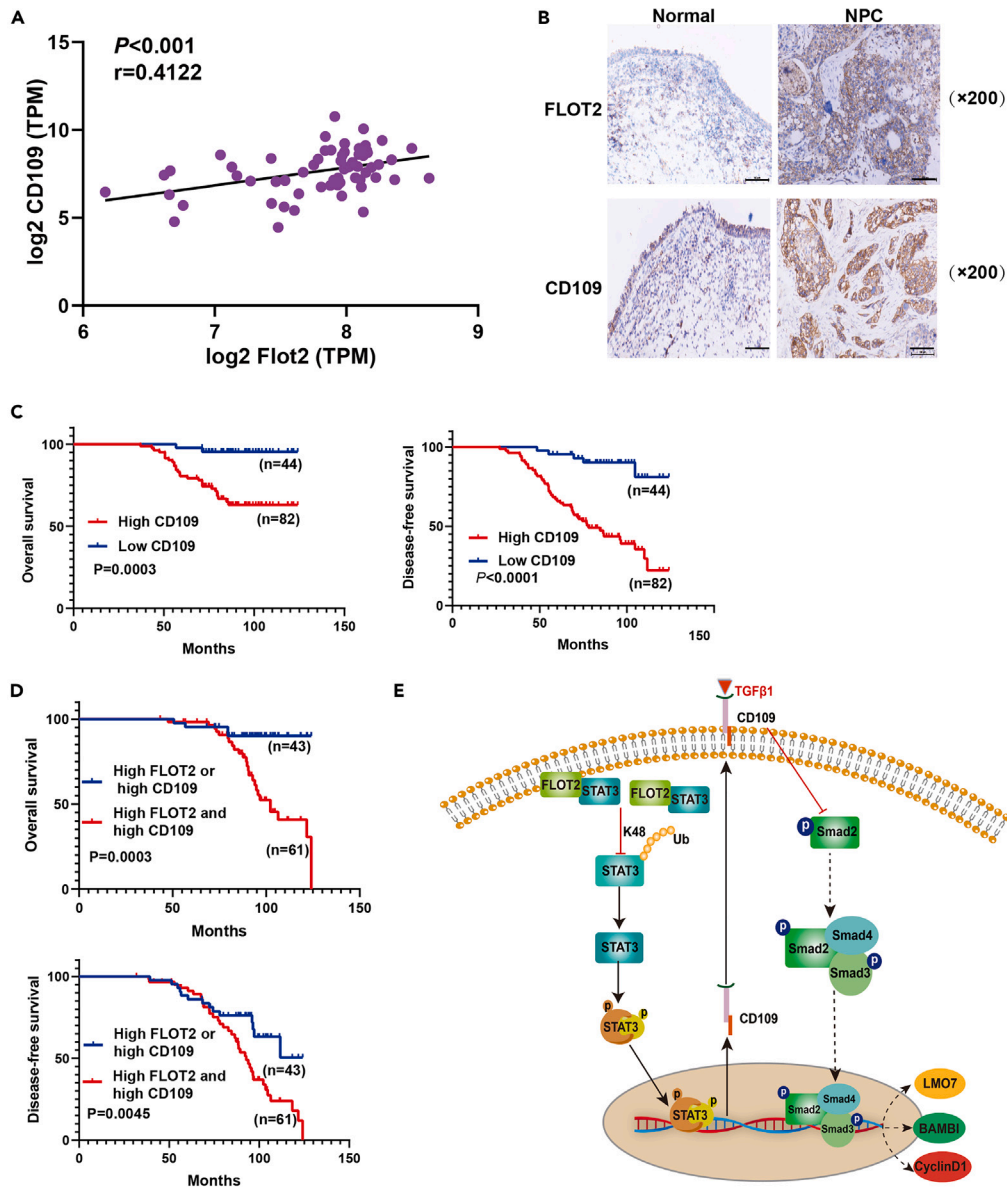


**Figure 6. FLOT2 expression is positively associated with CD109 level in NPC**

(A) Positive correlation between FLOT2 and CD109 expression in NPC tissues of a GEO batch.

(B) Representative IHC images of FLOT2 and CD109 expression in NPE and NPC samples. Scale bar, 100  $\mu$ m.

(C) Kaplan Meier survival analysis for NPC patients based on expression levels of CD109.

(D) Kaplan Meier survival analysis for NPC patients based on expression levels of both FLOT2 and CD109.

(E) Mechanism diagram in this study. FLOT2 promotes NPC progression by suppressing TGF- $\beta$  signaling via stimulating the expression of CD109 by stabilizing STAT3.

- lung cancer state reveals a targetable CD109-Janus kinase-Stat axis. *Nat. Med.* 23, 291–300.
- Kim, J.S., Shin, M.J., Lee, S.Y., Kim, D.K., Choi, K.-U., Suh, D.-S., Kim, D., and Kim, J.H. (2023). CD109 Promotes Drug Resistance in A2780 Ovarian Cancer Cells by Regulating the STAT3-NOTCH1 Signaling Axis. *Int. J. Mol. Sci.* 24, 10306.
  - Lin, Y., Zhou, X., Yang, K., Chen, Y., Wang, L., Luo, W., Li, Y., Liao, J., Zhou, Y., Lei, Y., et al. (2021). Protein tyrosine phosphatase

receptor type D gene promotes radiosensitivity via STAT3 dephosphorylation in nasopharyngeal carcinoma. *Oncogene* 40, 3101–3117.

- Mohassab, A.M., Hassan, H.A., Abdelhamid, D., and Abdel-Aziz, M. (2020). STAT3 transcription factor as target for anti-cancer therapy. *Pharmacol. Rep.* 72, 1101–1124.
- Peng, D., Fu, M., Wang, M., Wei, Y., and Wei, X. (2022). Targeting TGF- $\beta$  signal

transduction for fibrosis and cancer therapy. *Mol. Cancer* 21, 104.

- Li, J., Wang, W., Chen, S., Cai, J., Ban, Y., Peng, Q., Zhou, Y., Zeng, Z., Li, X., Xiong, W., et al. (2019). FOXA1 reprograms the TGF- $\beta$ -stimulated transcriptional program from a metastasis promoter to a tumor suppressor in nasopharyngeal carcinoma. *Cancer Lett.* 442, 1–14.
- Zhang, J.-M., Murakumo, Y., Hagiwara, S., Jiang, P., Mii, S., Kalyoncu, E., Saito, S.,

- Suzuki, C., Sakurai, Y., Numata, Y., et al. (2015). CD109 attenuates TGF- $\beta$ 1 signaling and enhances EGF signaling in SK-MG-1 human glioblastoma cells. *Biochem. Biophys. Res. Commun.* 459, 252–258.
38. Bizet, A.A., Liu, K., Tran-Khanh, N., Saksena, A., Vorstenbosch, J., Finnson, K.W., Buschmann, M.D., and Philip, A. (2011). The TGF- $\beta$  co-receptor, CD109, promotes internalization and degradation of TGF- $\beta$  receptors. *Biochim. Biophys. Acta* 1813, 742–753.
39. Litvinov, I.V., Bizet, A.A., Binamer, Y., Jones, D.A., Sasseville, D., and Philip, A. (2011). CD109 release from the cell surface in human keratinocytes regulates TGF- $\beta$  receptor expression, TGF- $\beta$  signalling and STAT3 activation: relevance to psoriasis. *Exp. Dermatol.* 20, 627–632.
40. Bizet, A.A., Tran-Khanh, N., Saksena, A., Liu, K., Buschmann, M.D., and Philip, A. (2012). CD109-mediated degradation of TGF- $\beta$  receptors and inhibition of TGF- $\beta$  responses involve regulation of SMAD7 and Smurf2 localization and function. *J. Cell. Biochem.* 113, 238–246.

STAR★METHODS

KEY RESOURCES TABLE

REAGENT or RESOURCE	SOURCE	IDENTIFIER
<b>Antibodies</b>		
Anti-FLOT2 antibody	Cell Signaling Technology	Cat# 3436, RRID:AB_2106572
Anti-FLOT2 antibody	Santa Cruz Biotechnology	Cat# sc-28320, RRID:AB_627618
Anti-CD109 antibody	Santa Cruz Biotechnology	Cat# sc-271085, RRID:AB_10610041
Anti-CD109 antibody	R and D Systems	Cat# AF4385, RRID:AB_2073929
Anti-GAPDH antibody	Santa Cruz Biotechnology	Cat# sc-47724, RRID:AB_627678
Anti-Smad2 antibody	Cell Signaling Technology	Cat# 5339, RRID:AB_10626777
Anti-p-Smad2 antibody	Cell Signaling Technology	Cat# 18338, RRID:AB_2798798
Anti-STAT3 antibody	Proteintech	Cat# 10253-2-AP, RRID:AB_2302876
Anti-p-STAT3 antibody	Cell Signaling Technology	Cat# 9145, RRID:AB_2491009
Anti-His antibody	Proteintech	Cat# 66005-1-Ig, RRID:AB_11232599
Normal Rabbit IgG	Cell Signaling Technology	Cat# 2729, RRID:AB_1031062
Anti-Ub antibody	Santa Cruz Biotechnology	Cat# sc-8017 AC, RRID:AB_2762364
Anti-Ki67 antibody	Proteintech	Cat# 27309-1-AP, RRID:AB_2756525
Anti-Rabbit IgG	Sigma-Aldrich	Cat# A0545, RRID:AB_257896
Anti-Mouse IgG	Sigma-Aldrich	Cat# A9044, RRID:AB_258431
Anti-Sheep IgG, Alexa Fluor 647	Abcam	Cat# ab150179, RRID:AB_2884038
Anti-Rabbit IgG, Alexa Fluor 488	Abcam	Cat# ab150077, RRID:AB_2630356
Anti-Rabbit IgG, Alexa Fluor 647	Abcam	Cat# ab150115, RRID:AB_2687948
<b>Biological samples</b>		
NPE and NPC tissues	Xiangya Hospital, Central South University	N/A
NPC microarray	Shanghai Superbiotek	NPC1401
<b>Chemicals, peptides, and recombinant proteins</b>		
CHX	AbMole	M4879
MG-132	MCE	HY-13259
SIS3	MCE	HY-13013
Matrigengel Matrix	Corning	354234
recombinant human TGF- $\beta$ 1 protein	Proteintech	HZ-1011
<b>Critical commercial assays</b>		
RevertAid First Strand cDNA Synthesis Kit	Thermo Scientific	K1622
AceQ qPCR SYBR Green Master Mix	Vazyme	Q131-02
ChIP kit	Abcam	ab500
Luciferase Assay System	Promega	E2920
<b>Deposited data</b>		
Raw and analyzed data	This paper	GEO : GSE245418
<b>Experimental models: Cell lines</b>		
Human: 5-8F	Cancer Research Institute, Central South University	N/A
Human: C666-1	Cancer Research Institute, Central South University	N/A

(Continued on next page)

**Continued**

REAGENT or RESOURCE	SOURCE	IDENTIFIER
Human: 6-10B	Cancer Research Institute, Central South University	N/A
<b>Experimental models: Organisms/strains</b>		
BALB/C nude mice (male)	Slake Jingda Experimental Animal Co., Ltd	N/A
<b>Oligonucleotides</b>		
shRNA targeting sequence for FLOT2, CD109, and Stat3, see <a href="#">Table S4</a>	This paper	N/A
Primers for qRT-PCR, see <a href="#">Table S5</a>	This paper	N/A
Primers for CHIP-PCR, see <a href="#">Table S6</a>	This paper	N/A
<b>Recombinant DNA</b>		
pRK5-HA-Ubiquitin-WT	Addgene	Cat# 17608, RRID:Addgene_17608
pRK5-HA-Ubiquitin-K48	Addgene	Cat# 17605, RRID:Addgene_17605
pRK5-HA-Ubiquitin-K63	Addgene	Cat# 17606, RRID:Addgene_17606
pLV-CD109	Vector Buidler	<a href="https://www.vectorbuilder.cn/popular-vectors/human-gene/cd109-135228.html">https://www.vectorbuilder.cn/popular-vectors/human-gene/cd109-135228.html</a>
shCD109	Vector Buidler	<a href="https://www.vectorbuilder.cn/popular-vectors/human-gene/cd109-135228.html">https://www.vectorbuilder.cn/popular-vectors/human-gene/cd109-135228.html</a>
pLV-FLOT2	Vector Buidler	<a href="https://www.vectorbuilder.cn/popular-vectors/human-gene/flot2-2319.html">https://www.vectorbuilder.cn/popular-vectors/human-gene/flot2-2319.html</a>
shFLOT2	Vector Buidler	<a href="https://www.vectorbuilder.cn/popular-vectors/human-gene/flot2-2319.html">https://www.vectorbuilder.cn/popular-vectors/human-gene/flot2-2319.html</a>
pLV-STAT3	Vector Buidler	<a href="https://www.vectorbuilder.cn/popular-vectors/human-gene/stat3-6774.html">https://www.vectorbuilder.cn/popular-vectors/human-gene/stat3-6774.html</a>
shSTAT3	Vector Buidler	<a href="https://www.vectorbuilder.cn/popular-vectors/human-gene/stat3-6774.html">https://www.vectorbuilder.cn/popular-vectors/human-gene/stat3-6774.html</a>
pEnter-STAT3-His	WZ Biosciences Inc	<a href="https://www.wzbio.com.cn/">https://www.wzbio.com.cn/</a>
<b>Software and algorithms</b>		
GraphPad Prism 8	GraphPad	N/A
SPSS 19.0	IBM	N/A

**RESOURCE AVAILABILITY****Lead contact**

The relevant experimental reagents, experimental methods, and related data of this study can be obtained by contacting Caiping Ren ([rencaiping@csu.edu.cn](mailto:rencaiping@csu.edu.cn)).

**Materials availability**

The study did not generate new unique reagents.

**Data and code availability**

The raw sequencing data for this study was uploaded into the GEO database. These data can be obtained at GEO database: dataset GSE245418.

This paper does not report the original code.

Any additional information required to reanalyze the data reported in this paper is available from the [lead contact](#) upon request.

**EXPERIMENTAL MODEL AND STUDY PARTICIPANT DETAILS****Clinical samples**

Firstly, to analyze the correlation between FLOT2 and CD109 mRNA levels in NPC tissues, we downloaded the dataset GSE53819 (NPE=18, NPC=18), dataset GSE12452 (NPE=10, NPC=31), and dataset GSE64634 (NPE=4, NPC=12) datasets with permission of the local Institutional

Review Board from the Gene Expression Omnibus Database (GEO) (<https://www.ncbi.nlm.nih.gov/geo/>). After gene reannotation and batch normalization, a new GEO batch containing 61 NPC samples, and 32 control tissues was generated. Furthermore, to detect the protein levels of FLOT2 and CD109 in NPE and NPC tissues, we collected the paraffin sections of NPE (n=50) and NPC (n=60) samples from Xiangya Hospital, Central South University with permission of the Clinical Medical Ethics Committee, Xiangya Hospital, Central South University (IRB NO. 2022101061). All patients wrote the informed consent. To further investigate the expression and prognosis value of FLOT2 and CD109 in NPC, tissue microarrays of NPC (n=126) were obtained from Shanghai Super Biotek (Shanghai, China) with permission of the local Institutional Review Board. The clinical data are shown in [Tables S1–S3](#).

### **In vivo experiments**

All of the animal experiments were approved by the Animal Care Committee of Central South University and followed the guidelines of the Institutional Animal Care and Use Committee (IRB NO. 2023030597). The nude mice (BALB/c, male, 18–20 g, 5–6 weeks) used in this study were purchased from the Animal Research Center of Central South University. For *in vivo* tumorigenesis, NPC cells ( $2 \times 10^6/0.2$  ml) were injected subcutaneously into the subaxillary region of the right forelimb. The tumor volume was equivalent to  $1/2$  (length  $\times$  width<sup>2</sup>). One month after injection, all mice were sacrificed to examine the final tumor weight and volume. To test the metastasis of NPC cells *in vivo*, cells ( $2 \times 10^6/0.2$  ml) were injected by the tail vein. After about 2 months, the mice were sacrificed and their lung tissues were detached. All of the dissected tissue samples were paraffin-embedded, sectioned, and stained with HE; the expression of related markers was stained by IHC and the lung metastasis nodes were counted.

## **METHOD DETAILS**

### **Cell culture, transfection, and treatment**

Human NPC cell lines 5-8F, C666-1, and 6-10B from our laboratory without mycoplasma contamination were cultured in RPMI 1640 medium, and the HEK293T cell line was cultured in DMEM medium, supplemented with 10% fetal bovine serum (Gibco) and 1% antibiotics (100 U/ml penicillin and 0.1 mg/ml streptomycin). All the cell lines were maintained at 37°C in 5% CO<sub>2</sub>. All the cell lines have been authenticated with the STR genotyping method. Plasmids contained pLV-shCD109, pLV-CD109, pLV-shSTAT3, pLV-STAT3, pLV-shFLOT2, pLV-FLOT2 pEnter-STAT3-His, and their corresponding control vectors, Ubiquitin-WT, K48, K63. The target sequences of shRNAs are described in [Table S4](#). NPC cells were infected with the indicated lentiviral reagent, or transfected with the indicated plasmid using PEI (Beyotime), and then selected using antibiotics.

### **Immunohistochemistry (IHC) and Hematoxylin and eosin (HE)**

For IHC assays, the paraffin-embedded slides were deparaffinized, performed for antigen retrieval, and blocked with a proper blocking solution. The slides were then incubated with the primary antibody overnight at 4°C. The next day, the slides were incubated with relative secondary antibodies at 37°C for 30 min, and stained with a DAB staining kit (#ZLI9017, ZSGB BIO). At last, the slides were rehydrated. The following antibodies were used for studies: anti-FLOT2 (1:30, #SC-28320, Santa Cruz); anti-CD109 (1:30, #SC-271085, Santa Cruz); anti-Ki67 (1:2000, #SC-28320, Proteintech).

For HE assays, the paraffin-embedded slides were deparaffinized, stained with hematoxylin-eosin, and rehydrated.

### **Cell viability assay**

For cell viability assay, cells were seeded into 96-well plates at  $1 \times 10^3$  cells per well. 10  $\mu$ l of Cell Counting Kit-8 (CCK-8) solution was added to the medium at 0, 24, 48, 72, and 96 h. Cells were incubated for 1 h. The absorbance at 450 nm was measured.

### **Cell cycle analysis by flow cytometry**

Cells were collected, fixed in 75% ethanol, and stored at -20°C. Fixed cells were treated with RNase A at 1 mg/ml for 30 min at 37°C, stained with 5  $\mu$ g/ml of propidium iodide (PI), and analyzed with FACSCalibur.

### **Transwell matrigel invasion and wound-healing assays**

For transwell matrigel invasion assays, cells suspended in the serum-free medium were added into the upper chambers coated with matrigel, and 10% FBS RPMI 1640 solution was added into the lower chamber. The chambers were fixed with 4% paraformaldehyde solution, stained with crystal violet, and counted under a microscope.

For wound-healing migration assays, cells were seeded into 6 well plates. The next day, the linear wound was generated using the 200  $\mu$ l pipette tip. The wound area was calculated with Image J Software.

### **Quantitative real-time polymerase chain reaction (qRT-PCR)**

Total RNA was extracted with the Trizol reagent. cDNA was synthesized with RevertAid First Strand cDNA Synthesis Kit (#K1622, Thermo Scientific). qRT-PCR detection was performed with SYBR Green Mix (#Q131-02, Vazyme). The primers were synthesized by Sangon (Shanghai, China) and described in [Table S5](#). mRNA expression was quantitated using the  $2^{-\Delta\Delta C_t}$  method.

### Western blot analysis

The total protein of cells was harvested with RIPA solution on ice for 30 min. The supernatant was collected by centrifuging for 30 min at 4°C, 12,000 rpm. The BCA method was used to measure the concentration of proteins. Sodium dodecyl sulfate-polyacrylamide gel electrophoresis (SDS-PAGE) was used to separate different weights of protein. The proteins were transferred to the PVDF membrane, and the membranes were blocked for 2 h with 5% BSA solution at room temperature. Then, the membranes were incubated with primary antibodies solution at 4°C overnight. The next day, after being washed with TBST solution, the membranes were incubated with relative secondary antibody solution for 2 h at room temperature, and visualized with a chemiluminescence reagent (Millipore). The following antibodies from various vendors were used for studies: anti-FLOT2 (1:1000, #3426, Cell Signaling Technology); anti-GAPDH (1:1000, #SC-47724, Santa Cruz); anti-CD109 (1:200, #SC-271085, Santa Cruz); anti-Smad2 (1:1000, #5339, Cell Signaling Technology); anti-p-Smad2 (1:1000, #18338, Cell Signaling Technology); anti-STAT3 (1:2000, #10253-2-AP, Proteintech); anti-p-STAT3 (1:1000, #9134, Cell Signaling Technology); anti-Ub (1:200, #SC-8017, Santa Cruz); anti-rabbit IgG (A0545) and anti-mouse IgG (A9044) (1:40,000, Sigma).

### Co-immunoprecipitation (Co-IP) assay

The total protein of cells was harvested with NP-40 solution. The concentration of proteins was measured with the BCA method. Then, relative antibodies were added to the solution, shake the mixture overnight at 4°C. The next day, 20-30 µl protein A/G beads (B23201, Bimake) were added to the solution, shake the mixture for 2 h at 4°C. Magnetic beads were collected, suspended with NP40 lysis and loading buffer, and denatured at 95°C for 5 min. Then the sample solution was collected by the Magnetic Separation Rack. Protein-protein interaction was detected with the Western blot method as mentioned above. The following antibodies were used for studies: anti-FLOT2 (#3426, Cell Signaling Technology); anti-STAT3 (#10253-2-AP, Proteintech); anti-His (#66005-1-Ig, Proteintech).

### Immunofluorescence staining

NPC cells were seeded into the cover slide of 24-well plates. The next day, cells were fixed with 4% paraformaldehyde for 5 min. 5% FBS was used to incubate cells for 1-2 h at room temperature. The cells were incubated with primary antibodies overnight at 4°C. Relative fluorescently labeled secondary antibodies were used to incubate cells at room temperature for 2 h in the dark. 5 µg/ml of DAPI solution was used to stain the cell nuclear. Pictures were collected with a laser scanning confocal microscope (ZEISS). The following antibodies were used for studies: anti-FLOT2 (1:30, #SC-28320, Santa Cruz); anti-STAT3 (1:50, #10253-2-AP, Proteintech); anti-CD109 (1:100, #AF4385, R and D Systems).

### Chromatin immunoprecipitation (ChIP) assay

The ChIP assays were performed according to the manufacturer's protocol (abcam, ab500). All PCR primers are listed in the Table S6. We used the anti-STAT3 (#10253-2-AP, Proteintech) to immunoprecipitate the chromatin.

### Dual-luciferase assay

The CD109 promoter regions including -2000 bp upstream of the transcription start site (TSS) were cloned into the pGL3-basic vector. A dual-luciferase system (Promega, USA) was used to measure firefly and renilla luciferase activities according to the manufacturer's protocol.

### RNA sequencing

Novogene Biotech Co., Ltd was used to perform RNA sequencing of 5-8F-control and 5-8F-shFLOT2 samples. RNA integrity was assessed using the RNA Nano 6000 Assay Kit of the Bioanalyzer 2100 system (Agilent Technologies, CA, USA). The sequencing procedure was generated on an Illumina Novaseq platform. Expression data and the differentially expressed mRNAs in 5-8F-control and 5-8F-shFLOT2 cells were performed using the DESeq2 R package (1.20.0). An enrichment analysis was conducted between 5-8F-control and 5-8F-shFLOT2 groups to investigate the potential KEGG pathways in the Gene set enrichment analysis (GSEA) website (<https://www.gsea-msigdb.org/gsea/downloads.jsp>). The original sequencing dataset supporting the results of this study is uploaded to the NCBI GEO database. These data are available at GEO database: dataset GSE245418.

## QUANTIFICATION AND STATISTICAL ANALYSIS

All the experimental data were presented as means ± standard deviation (SD). Analyses were performed by using GraphPad Prism Software 8.0 and SPSS 19.0. Student t-test was used for comparing two groups, and One-way ANOVA was applied for comparing multiple groups. Spearman correlation coefficient was used to assay the correlation between FLOT2 and CD109 expression. Kaplan-Meier analysis was performed to produce overall survival (OS) and disease-free survival (DFS) curves and the log-rank test was used to calculate *p*-values. \**p* < 0.05, \*\**p* < 0.01 and \*\*\**p* < 0.001 were considered statistically significant.